Static characteristics of the new artificial pneumatic muscle

Jakub Takosoglu[1,*]

[1]Faculty of Mechatronics and Mechanical Engineering, Department of Manufacturing Engineering and Metrology, Kielce University of Technology, Aleja Tysiaclecia Panstwa Polskiego 7, 25-314 Kielce, Poland

Abstract. The pneumatic artificial muscles are used as driving elements of mobile, anthropomorphic, bionic and humanoid robots as well as rehabilitation and physiotherapeutic manipulators. The PAMs are also increasingly used for the automation of industrial processes. The article presents test stands and methods used to determine the static, isobaric, isotonic and isometric characteristics of the new pneumatic artificial muscles. The muscles have been designed and developed at the Kielce University of Technology. Comparative tests of technical parameters of the designed muscle with the muscles available on the market have been performed.

1 Introduction

The pneumatic artificial muscles belong to a group of pulling single-acting pneumatic actuators. They are characterized by low consumption of compressed air, are completely sealed, can work in contaminated and harmful environments, even underwater [1]. They generate much greater force with the same operating and technical parameters in relation to the standard pneumatic actuators. They are very durable and cheap to operate (no moving parts). There are only two products on the pneumatic industry market: Festo – Fluidic Muscle MAS and DMSP muscles, and Shadow Robot Company – Shadow Air Muscle SAM muscles (Fig, 1).

Fig. 1. Festo – Fluidic Muscle DMSP muscle and Shadow Robot Company – Shadow Air Muscle SAM muscle.

The Festo muscles are more popular due to their marketing campaigns and very good technical support. The book [2] published by Festo presents 99 examples of applications in industrial processes for pneumatic muscles. Festo has also implemented several bionic projects with pneumatic muscles, which were presented at the largest trade fair in the world. Due to the design and the simple structure, the pneumatic artificial muscles are the subject of many scientific works [3–12]. The article [13] presents a broad review of pneumatic muscles developed between 1930 and 2005. Fig. 2 shows the Pneumatic Artificial Muscles PAM-20-330 (under pressure, normal and relaxed) developed at the Kielce University of Technology.

Fig. 2. The pneumatic artificial muscles PAM made at the Kielce University of Technology: a) general view, b) connection.

Table 1 shows the technical parameters of the PAM-20-330, MAS-10-300, S30AM-S-1 pneumatic artificial muscles.

Table 1. Technical parameters of the pneumatic artificial muscles.

Parameter	**Value**		
	Festo Fluidic Muscle	Shadow Air Muscle	Kielce University of Technology Muscle
Symbol	MAS-10-300	S30AM-S-1	PAM-20-330
Mode of operation	Single-acting, pulling	Single-acting, pulling	Single-acting, pulling
Internal diameter D_n	10 mm	19 mm	20 mm
Internal diameter when fully contracted* D_{min}	8.7 mm	15 mm	33.0 mm
Internal diameter when fully extended* D_{max}	20.4 mm	30 mm	12.7 mm
Nominal length L_n	300 mm	173 mm	330 mm

* Corresponding author: qba@tu.kielce.pl

Length of the muscle when fully contracted* L_{min}	252 mm	152 mm	290 mm
Length of the muscle when fully extended* L_{max}	306 mm	213 mm	410 mm
Max. operating pressure p	8 bar	3.5 bar	5 bar
Max. permissible pre-tensioning** ε_{min}	-2 % of L_n	-23.1 % of L_n	-24.2 % of L_n
Max. permissible contraction** ε_{max}	*16 % of L_n*	28.6 % of L_{max}	29.3 % of L_{max}
Lifting force at max. permissible operating pressure F_{max}	630 N	700 N	775 N
Max. additional load, freely suspended	30 kg	-	-
Operating frequency f	35 Hz	210 Hz	-
Max. hysteresis	3% of nominal length	-	-
Max. relaxation	4% of nominal length	-	-
Repetition accuracy	1% of nominal length	-	-
Ambient temperature	-5°C+60°C	0°C+50°C	-
Contraction times	-	0.1-0.5 s	-

The designed and produced muscle is a rubber bladder surrounded by a plastic braided mesh sleeve. The muscle connections are sealed threaded joints with bladder clamped at the ends. Slightly modified standard hydraulic elements sized ½" were used in the design. In order to prevent cutting the muscle during clamping, special plastic inserts were made on 3D printers using the additive manufacturing technology. The inserts were placed between the joint and the bladder. Before the clamping, the bladder was pre-extended to increase the relative contraction and to minimize the hysteresis effect. Thanks to the use of generally available parts, the cost of the muscle production is several times lower than the muscles available on the market from professional companies.

2 Test stand

The technical parameters as well as static and dynamic characteristics of the pneumatic artificial muscles are extremely important for their application. To determine the static characteristics, a test stand was designed, the diagram of which is shown in Fig. 3, while Fig. 4 shows its general view.

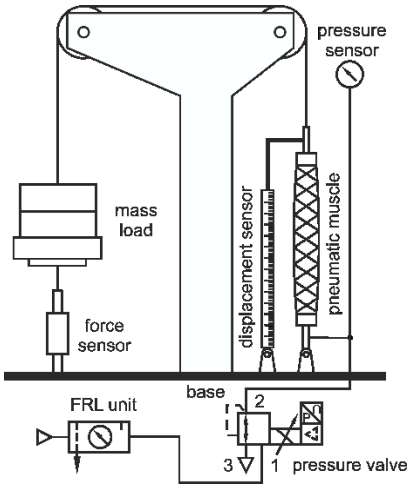

Fig. 3. Diagram of the test stand.

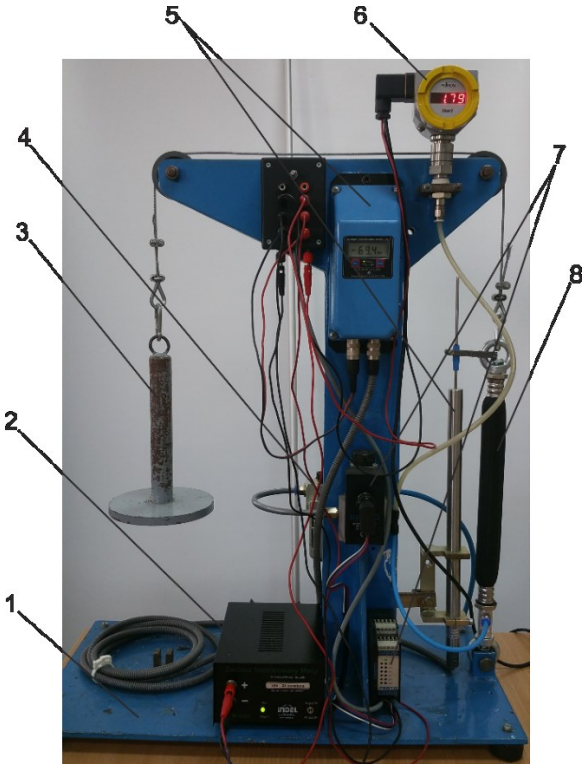

Fig. 4. General view of the test stand: 1 – base, 2 – power supply, 3 – mass load, 4 – FRL (Filter-Regulator-Lubricator) unit, 5 – displacement sensor, 6 – pressure sensor, 7 – proportional pressure valve, 8 – pneumatic artificial muscle.

A non-symmetrical T-shaped arm was mounted on a steel base. Two pulleys, cooperating with a steel wire, were mounted in the arm. One end of the muscle was attached to the base, while the steel wire was attached to the other end. The wire was passed through the pulleys and the other end was connected to the mass load. A displacement sensor was mounted axially to the pneumatic artificial muscle. A proportional pressure valve was used to control the muscle, and a pressure sensor was used to measure the pressure inside the muscle. A force sensor is installed between the mass load in order to determine the pulling force of the muscle. The stand allows to determine the static characteristics: isobaric, isotonic and isometric of the pneumatic artificial muscles. To determine the static

characteristics it is necessary to calculate the relative contraction. To calculate the relative contraction, the following relationships were developed [13]:

$$\varepsilon = \frac{L_{max}-L}{L_{max}} \cdot 100\% \,, \qquad (1)$$

$$\varepsilon_{min} = \frac{L_n-L_{max}}{L_n} \cdot 100\% \,, \qquad (2)$$

$$\varepsilon_{max} = \frac{L_{max}-L_{min}}{L_{max}} \cdot 100\% \,, \qquad (3)$$

where:
L – actual length of the muscle,
L_n – nominal length of the muscle,
L_{max} – length of the muscle when fully extended,
L_{min} – length of the muscle when fully contracted.

3 Experimental data

The contraction ε, depending on the pulling force F resulting from the mass load, is measured to determine the isobaric characteristics $F=f(\varepsilon)$ of the pneumatic artificial muscle at constant pressure $(p=const)$ inside the muscle. The principle of determining the isobaric characteristics is shown in Fig. 5.

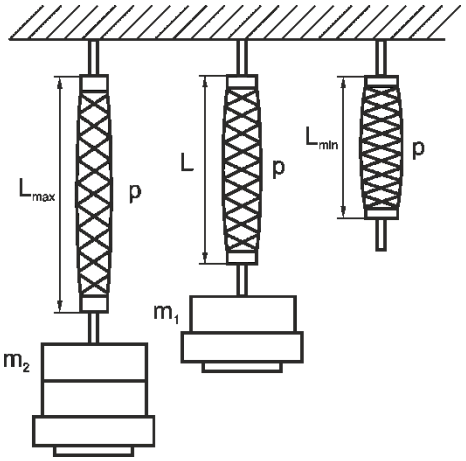

Fig. 5. The principle of determining the isobaric characteristics of the pneumatic artificial muscle.

The isobaric characteristics are limited by a maximum pulling force of 775N at the max. permissible pre-tensioning, at which max. stretching is ε_{min}=-24.2% of L_n n, the max. contraction is ε_{max}=29.3 % of L_{max} and max. working pressure is p_{max}=0.5 MPa. Fig. 6 shows the obtained isobaric characteristics of the pneumatic artificial muscle PAM-20-330.

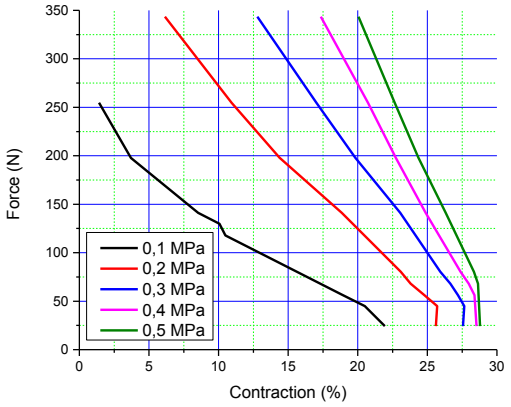

Fig. 6. The isobaric characteristics of the pneumatic artificial muscle PAM-20-330.

The principle of determining the isotonic characteristics $\varepsilon=f(p)$ of the pneumatic muscle is shown in Fig. 7.

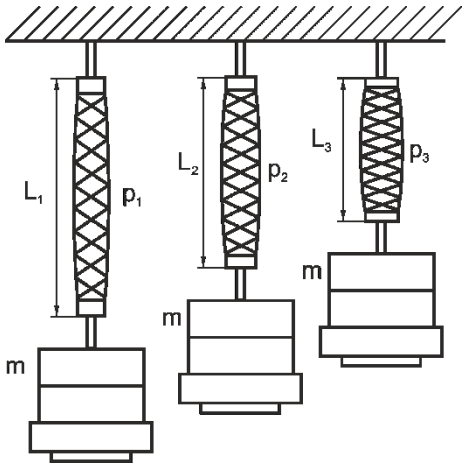

Fig. 7. The principle of determining the isotonic characteristics of the pneumatic artificial muscle.

The relative contraction ε is measured depending on the pressure p inside the muscle and with constant muscle strain $(F=const)$. The isotonic characteristics are limited by the max. permissible relative contraction ε_{max}=29.3% and the max. permissible relative stretching ε_{min}=-24.2%. Fig. 8 shows the obtained isotonic characteristics of the pneumatic artificial muscle PAM-20-330.

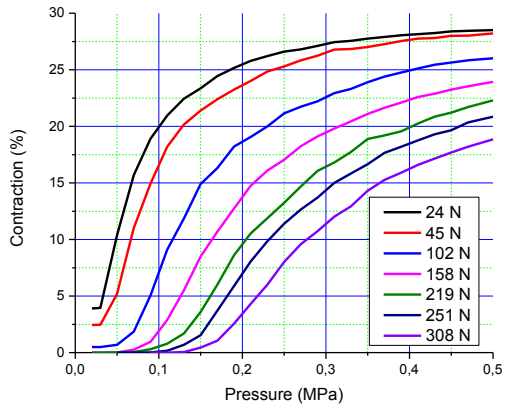

Fig. 8. The isotonic characteristics of the pneumatic artificial muscle PAM-20-330

The principle of determining the isometric characteristics ΔF=f(p) of the pneumatic muscle is shown in Fig. 9.

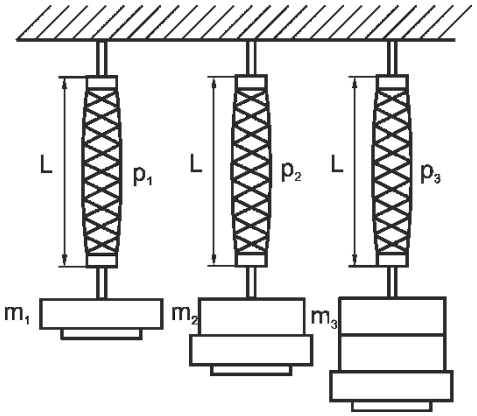

Fig. 9. The principle of determining the isometric characteristics of the pneumatic artificial muscle

The change in pressure p inside the pneumatic muscle and the change in muscle tension ΔF are measured at constant contraction (ε=const). Fig. 10 shows the obtained isometric characteristics of the pneumatic artificial muscle PAM-20-330.

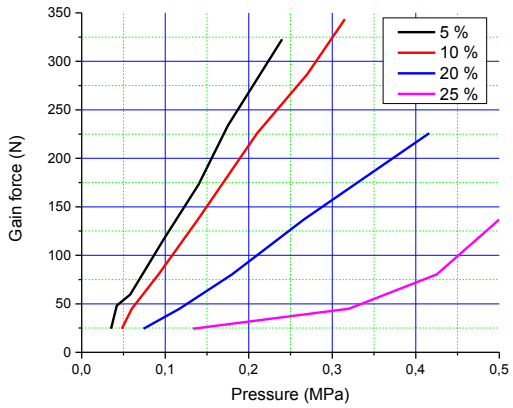

Fig. 10. The isometric characteristics of the pneumatic artificial muscle PAM-20-330.

4 Summary

The work presents the experimental data on the new artificial pneumatic muscle PAM-20-330 designed and developed at the Kielce University of Technology. The test stands and methods used to determine the static, isobaric, isotonic and isometric characteristics are presented here. The PAM-20-330 muscle achieves better technical and performance parameters compared to the muscles offered by the leading manufacturers of the pneumatic industry. The PAM-20-330 has a high pulling force of F=775N at a supply pressure of 0.5MPa. The hysteresis effect was minimized due to the pre-tensioning of the bladder. As in the case of the Shadow Air Muscle by Shadow Robot Company, the pre-stretching is eliminated by the use of a rectilinear bladder. The designed PAM muscle is also characterized by very good static characteristics. The presented characteristics can be successfully compared with the characteristics of the MAS and DMSP type muscles, as a specially developed formula was used to calculate the relative contraction. This type of static characteristics for the bladder-type muscles are presented for the first time and are not found in the available literature.

References

1. J.E. Takosoglu, (Inst. Thermomechanics, Acad. Sci. Czech Republic, Prague, 2017)
2. S. Hesse, (Festo AG & Co., Esslingen, 2001)
3. F. Daerden, D. Lefeber, B. Verrelst, R. Van Ham, (2001)
4. F. Daerden, D. Lefeber, *Eur. J. Mech. Environ. Eng.* **47**, (2000)
5. I. Gaiser, in: R. Wiegand (Ed.), IntechOpen, Rijeka, 2012: p. Ch. 22
6. G.K. Klute, J.M. Czerniecki, B. Hannaford, *Int. J. Rob. Res.* **21**, 4 (2002)
7. D.S. Pietrala, (Inst. Thermomechanics, Acad. Sci. Czech Republic, Prague, 2016)
8. J.E. Takosoglu, (Inst. Thermomechanics, Acad. Sci. Czech Republic, Prague, 2016)
9. B. Verrelst, R. Van Ham, B. Vanderborght, D. Lefeber, F. Daerden, M. Van Damme, *Adv. Robot.* **20**, 7 (2006)
10. N. Yee, G. Coghill, (Auckland, New Zeland, 2002)
11. Z. Zhang, M. Philen, *J. Intell. Mater. Syst. Struct.* **23**, 3 (2011)
12. P.A. Laski, J.E. Takosoglu, S. Blasiak, (Brno Univ. Brno Univ. Technol., Inst. Solid Mechan. Mechatron. & Biomechan., 2014)
13. J.E. Takosoglu, P.A. Laski, S. Blasiak, G. Bracha, D. Pietrala, *Meas. Control*. **49**, 2 (2016)